



Shahid Chamran  
University of Ahvaz

# Journal of Applied and Computational Mechanics



Research Paper

## Numerical Study of the Hydrodynamic Behavior of an Archimedes Screw Turbine by Experimental Data in order to Optimize Turbine Performance: The Genetic Algorithm

Mohsen Zamani<sup>✉</sup>, Rouzbeh Shafaghat<sup>✉</sup>, Behrad Alizadeh Kharkeshi<sup>✉</sup>

Department of Mechanical Engineering, Babol Noshirvani University of Technology, Shariati Ave, Babol, 4714873113, Iran  
Email: mohsenzamanimec@yahoo.com (M.Z.); rshafaghat@nit.ac.ir (R.S.); b.alizadeh@nit.ac.ir (B.A.K.)

Received March 03 2023; Revised May 16 2023; Accepted for publication June 11 2023.

Corresponding author: R. Shafaghat (rshafaghat@nit.ac.ir)

© 2023 Published by Shahid Chamran University of Ahvaz

**Abstract.** Renewable energy could solve the problems caused by fossil fuels. The Archimedes hydro screw turbine is a potential tool for generating power from river currents. In this paper, a turbine at a scale of 1:6 has been made. It is installed and tested at various flow rates. The system is optimized using a genetic algorithm to achieve maximum efficiency. Due to the limitations that existed for conducting experimental tests at the optimal flow rate, the turbine at optimal flow rate is studied by CFD. In the turbine numerical simulation, the hydrodynamic characteristics of the turbine, such as rotational speed, power, torque, efficiency, and power coefficient are compared in the optimal flow rate (2.6 (lit/s)) and a flow rate of 2.4 (lit/s) (the closest flow rate to the optimal one). The results show that these values are higher in the optimal flow rate. Furthermore, the behavior of the turbine in these two conditions is compared using velocity, vorticity, pressure, and phase contours, which indicates that the velocity and pressure values are higher, and the vorticity and immersion values are lower in the optimal flow rate. Finally, for economic analysis of operating the turbine at the prototype scale as a hydropower plant, the discounted payback period for the turbine is determined, which varies between 2.55 to 5.93 years depending on the discount rate. It is also shown that operating this turbine at the prototype scale as a hydropower plant in Iran leads to currency savings of 1561 \$.

**Keywords:** Archimedes hydro screw turbine, Optimization, Genetic Algorithm, Numerical study, Economic study.

### 1. Introduction

Renewable energies are energy sources that are derived from natural resources that can replenish themselves in less than a human's lifetime without depleting the resource. Unlike fossil fuels, which are only available in limited quantities and will eventually run out as the extraction process continues, renewable resources are practically inexhaustible. More importantly, they cause little damage to the environment. Although produced through natural processes, fossil fuels do not regenerate as quickly as they are consumed. Despite the availability of renewable energy sources, the world still heavily relies on fossil fuels. Unfortunately, the pollution created by fossil fuels has reached unprecedented levels. Greenhouse gases produced by these fuels destroy the climate, and contaminated particles pose significant risks to human health [1]. Among renewable energies, hydropower is considered one of the best sources and has more resources worldwide compared to many other renewable energy sources, including solar and wind [2]. The Archimedes hydro screw turbine can be utilized as a small-scale hydropower plant to generate power from river flow. This type of turbine is a modernized version of an old device that has been used for pumping water for many years. The turbine is made up of a central cylinder connected to some spiral blades that are typically installed at a specific angle to the horizon. Water flow enters the top of the turbine and passes through the gaps between the blades, which causes the turbine to turn. The water then exits from the bottom end of the turbine. Connecting a generator to the turbine makes it possible to generate electricity from this mechanical rotation. Unlike most turbines, Archimedes screw turbines can be used in flows with low heads and low flow rates while still maintaining high efficiency [3]. Also, another advantage of these turbines compared to other hydro turbines is that due to the space between its blades, fishes can easily pass through it and there will be no problem in their lives [4].

Due to the various uses and applications that Archimedes screw has had over the years, many studies have been done on their different condition of operation. Rorres [5] with the aim of optimal design of Archimedes screw turbine geometry, determined optimal dimensionless ratios for screw turbines by different numbers of blades. Schleicher [6] investigated the performance of Archimedes screw turbine with a different pitch using Ansys Fluent software. He used the MRF method to move the turbine. The results showed that the rotational speed of the turbine compared to the head of the turbine has less effect on the turbine's efficiency. Waters [7] by using CFD investigated the effect of various parameters such as diameter ratio, length and pitch on the output torque of the Archimedes screw turbine. In this study, the diameter ratio had the greatest effect on the output



torque, and by reducing the diameter ratio, the output torque increased. Because by reducing the inner diameter, more water enters the buckets, and more pressure is created to turn the turbine. Lee et al. [8] used a 3D printer to construct the turbine due to the complex geometry of the Archimedes screw turbine. The manufactured turbine was made of polylactic, so the cost of its construction was lower than the use of metals. The results of the experimental tests have acceptable accuracy with the analytical model. Saroinsong et al. [9] studied the effect of vortex current on turbine performance. They stated that the vortex current can affect the turbine's performance and reduce its efficiency. They also stated that the vortex current would reduce the turbine's rotational speed. Lsicki et al. [10] optimized the results with the Bayesian method with the aim of optimal design and achieving the maximum efficiency of the turbine at a specific installation angle. By achieving the optimal installation angle, they could improve the turbine's performance. Songin [11] By experimental tests on different models of Archimedes screw turbine, stated that immersion at the end of the turbine causes the bucket to be reduced or removed, and as a result, the length of the turbine is short, which reduce output power and efficiency of the turbine. Kuzyn and Lubitz [3] investigated the losses in the turbine bearings and the immersion at the end of the Archimedes screw turbine. They explained these losses as the reason for the low efficiency of the turbine in experimental tests. Submersion and frictional losses were investigated using concepts related to open water channel and Darcy-Weisbach equations. Abdul Salam et al. [12] used Ansys Fluent software to investigate the effects of changing inlet flow rate, turbine placement angle and the number of blades on turbine torque, power and efficiency. Flow rate changes had a direct effect on these parameters. Also, this result was showed that with the increase in the number of blades, the torque and efficiency increase, but this increase is not high. Simmons [13] numerically investigated the Archimedes screw turbine using OpenFoam software and introduced various leaks for this turbine. He used RANS equations, SST k-omega model and VOF model for his numerical simulations. Dellinger et al. [14] numerically investigated the effect of the number of blades and installation angle on turbine performance. This numerical study was done using Ansys Fluent software. In their simulation, they also used k-omega SST models as turbulence models and VOF models for free surface. They concluded that turbine efficiency decreases at high angles due to the increase of turbine leaks. Montilla et al. [15] investigated the Archimedes screw turbine numerically using simulation in Ansys Fluent software. They compared the power coefficient for an inclined axis Archimedes screw turbine with a horizontal axis Archimedes screw turbine. They concluded that the inclined axis turbine would have higher power coefficient values and, as a result, would perform better than the horizontal axis turbine. Martinez et al. [16] to improve the design of the Archimedes screw turbine, analyzed the performance of this turbine. They said that to improve the performance of the turbine, the turbine leakage should be minimized. Alkistis and Stergiopoulos [17] numerically investigated the feasibility of using the Archimedes screw turbine to generate power from the river current in Greece. This study was done using Flow 3D software. The results have predicted power production in the amount of several terawatts (according to the available water resources) per year. Lee and Lee [18] concluded by examining a sample of Archimedes screw turbine that increasing the speed of the input flow to the turbine increased the rotational speed and torque values. Then they generalized the results of this laboratory sample for the prototype scale turbine. Shahvardi et al. [19] used CFD to investigate the rotational speed, inlet flow rate, and installation angle for the Archimedes screw turbine. By creating proper meshing and achieving 5 million cells for simulation, they achieved results with appropriate accuracy compared to experimental tests. Darmono and Pranoto [20] simulated turbine in order to achieve the effect of changing the number of turbine blades on its performance. They stated that the torque and output power of the turbine increases with the increase in the number of blades, but they did not consider the limitations and costs related to the construction of a turbine with a large number of blades. Zhang et al. [21] investigated various parameters of turbine. They found out the effect of the turbine installation angle on its rotational speed. They did multi-objective optimization by using Neural Network and Genetic Algorithm methods in order to achieve the optimal rotational speed at the best angle for optimal turbine design. With this method, they were able to increase the values of performance characteristics of the turbine. Adhikari et al. [22] conducted a simulation of a turbine using Ansys software. They used the SST k-omega model as the turbulence model. They stated that the number of blades may affect the inner radius of the turbine. Additionally, they observed that changes in the turbine's torque are directly and linearly related to the input flow rate. Ubando et al. [23] studied Archimedes screw turbines to evaluate the effective parameters in their design and various manufacturing methods. They stated that turbines produced using CNC machines or 3D printers have the capability to generate more power compared to ancient method. Zamani et al. [24] by experimentally investigating an Archimedes screw turbine model, generalized the experimental results for the prototype scale turbine by using Froude scaling. They also studied the operation of the prototype-scale turbine as a hydroelectric power plant from an economic point of view. Nugraha et al. [25] experimentally studied immersion in the turbine outlet. They concluded that with the increase of immersion, the output power and efficiency of the turbine decreases.

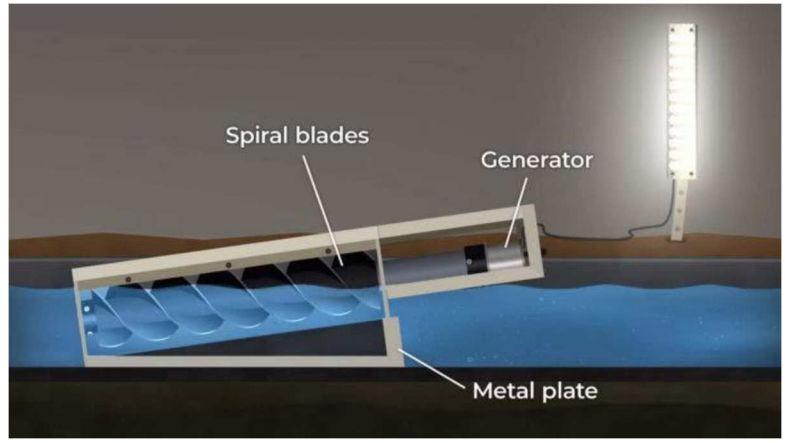
According to the past studies, it is clear that fewer studies have been done on the performance of the turbine in order to achieve the optimal efficiency. For this purpose, at first, an Archimedes screw turbine with optimal geometrical characteristics was built and experimental tests were conducted with the aim of investigating the effect of flow rate and electrical resistance on the performance characteristics of the turbine [24]. Then, the results obtained from the experimental tests were optimized by Genetic Algorithm to achieve the maximum efficiency of the turbine. By achieving the optimal flow rate of the turbine performance, due to the impossibility of conducting experimental tests in this flow rate, the turbine's performance at the optimal flow rate was evaluated numerically with the help of simulation in Star CCM+ software. Numerical simulation results were first validated using experimental and numerical results for the closest flow rate to the optimal flow rate. Finally, the results were compared in these two cases. At the end, the operation of the turbine in the prototype scale (6 times of the laboratory model) as a hydroelectric power plant is analyzed economically and the values of the discount payback period and currency savings for this turbine are determined in the prototype scale.

## 2. Experimental Study

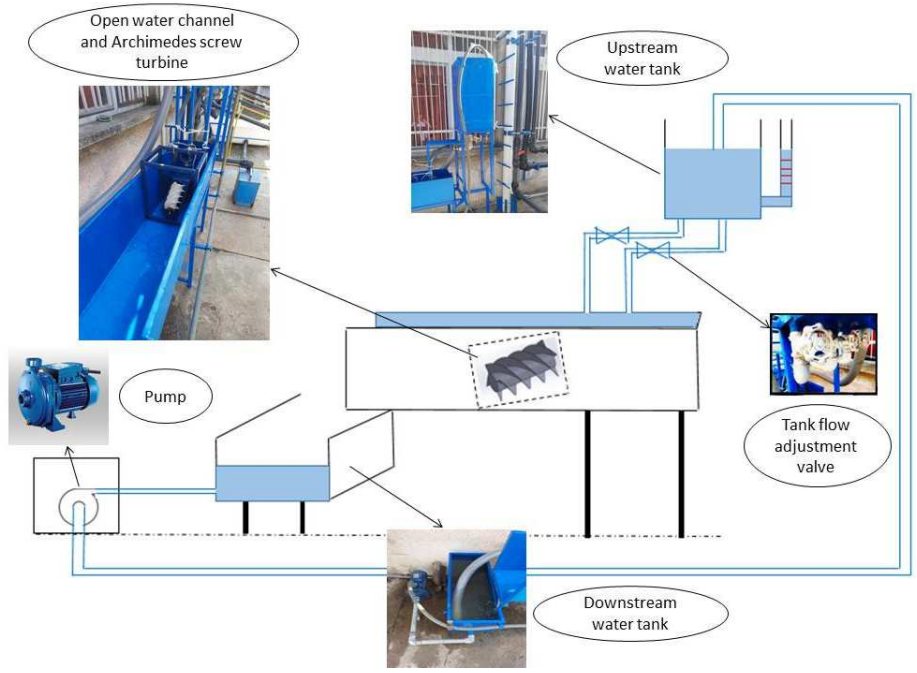
Figure 1 (a) shows a view of the Archimedes screw turbine. In this figure, the operation and different parts of this turbine are shown. Also, Figure 1 (b) shows the experimental setup for testing the Archimedes screw turbine in this paper. This site includes two water tanks, a pump, three valves and an open water channel. Water flows from the upstream water tank (by opening valves and setting the objective flow rate) to the downstream water tank through an open water channel where the Archimedes screw turbine is installed. It rotates the turbine and power is produced by the rotation of the generator. A pump is also used to pump water to the upper tank and also a drain pipe has also been installed to prevent the tank from overflowing. Also, Figure 1 (b) shows a view of the Archimedes screw turbine. In this figure, the operation and different parts of this turbine are shown.

Figure 2 shows the Archimedes screw turbine studied in this paper and its geometric characteristics. This turbine's design was done using the model provided by Rorres [5] and was made using 3D printer technology. Construction this turbine by using a 3D printer can better apply the details of the designed model to the manufactured sample than other turbine manufacturing methods. An FDM model printer is used to construction the turbine. This printer has a stroke length of 300 (mm) in different directions. This printer has made the turbine with 100 ( $\mu\text{m}$ ) accuracy by using ABS materials.





(a)



(b)

Fig. 1. a) Schematic view of a sample of Archimedes screw turbine b) Schematic view of placement and experimental installation Archimedes screw turbine in the laboratory [24, 26].

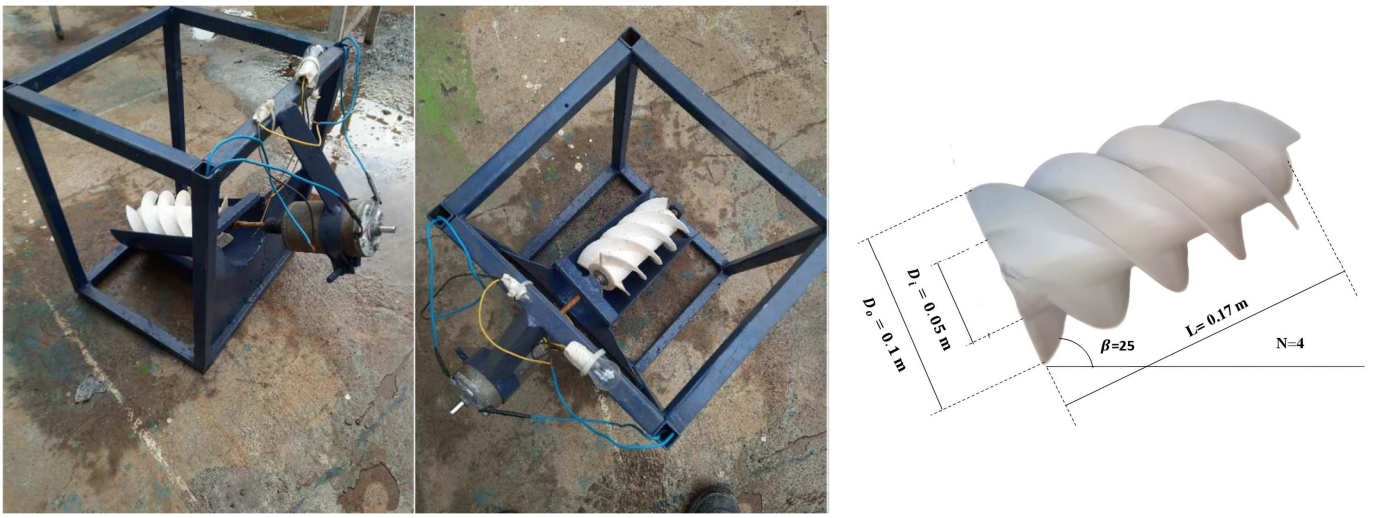


Fig. 2. Archimedes screw turbine and its geometrical characteristics.



Table 1. Design of experiment [24].

Flow rate (lit/s)	Resistance (Ohm)	Flow rate (lit/s)	Resistance (Ohm)	Flow rate (lit/s)	Resistance (Ohm)
	10		10		10
	20		20		20
1.2	30	2.4	30	3.6	30
	40		40		40
	50		50		50

2.1 Governing equations

For turbine power calculations, like all hydro turbines, first the total power value will be according to equation (1) [27]:

$$P_{in} = \rho g Q h \tag{1}$$

Also, equation (2) used to calculate efficiency [28]:

$$\eta = \frac{P_{out}}{P_{in}} \tag{2}$$

The output power is calculated according equations (3) and (4) [29]. In this paper, power calculations are done electrically according to the electric circuit connected to the generator:

$$P_{out_{mec}} = T \omega \tag{3}$$

$$P_{out_{elec}} = V.I \tag{4}$$

Also, the limit of rotational speed of turbine is shown by equation (5) [24]:

$$n = \frac{0.85}{D^{2/3}} \tag{5}$$

And, power coefficient of the turbine is calculated by equation (6) [30]:

$$C_p = \frac{P}{\rho n^3 D^5} \tag{6}$$

2.2 Design of experiment

According to Fig. 1, the test device is designed to change the flow rate for three different flow rates. Also studying the turbine's performance should be possible according to the consumption load. Therefore, the turbine performance was also studied for five electrical resistances. A total of 75 tests (considering uncertainty analysis and repeating each test 5 times) [24] should be performed on the turbine's performance, the uncertainty analysis results has been published in the previous paper of the authors [31].

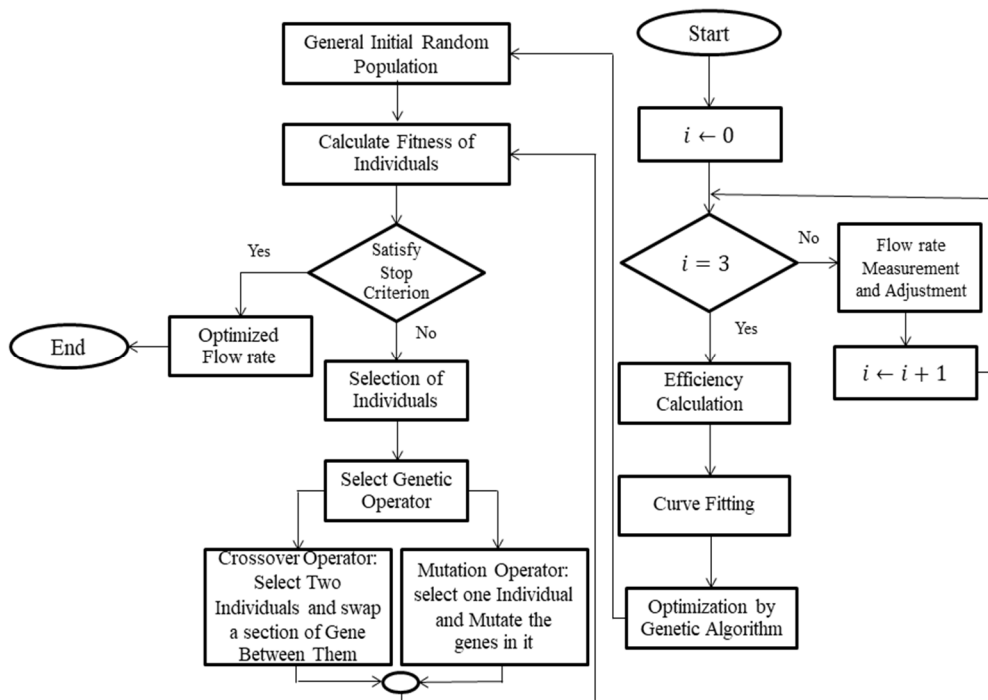


Fig. 3. Genetic algorithm flowchart [32].



### 3. Optimization by Genetic Algorithm

The aim of optimizing the results of experimental tests is to reach the maximum achievable efficiency for the Archimedes screw turbine. Genetic algorithm is used for this purpose. This algorithm stores possible answers or candidate answers for a particular problem in a chromosome-like data structure. In many cases, genetic algorithms are called function optimization algorithms. The execution of this algorithm usually starts with the generation of a population of chromosomes. Next, the generated data structures are evaluated, and the chromosomes that can display the optimal solution of the problem in a better way have more chances to reproduce than the weaker solutions. To optimize the results using the genetic algorithm for achieving maximum efficiency and optimal flow rate at which the turbine achieves maximum efficiency, MATLAB software can be used. MATLAB's optimization toolbox has the capability to provide the genetic algorithm as an optimizer function, which can be used to extract optimal values for the turbine. To do this, firstly, the equation related to the fitting curve of the efficiency diagram can be extracted from the CFTool toolbox of MATLAB. Then, by putting this equation as the input function for optimization, the optimization of the flow rate parameter can be carried out. After determining the optimized parameter, the optimization range can be specified, which can be approximately extracted from the diagram related to the turbine efficiency. Finally, by specifying other settings such as the number of initial selection chromosomes, determining the termination conditions of optimization, and other operators, maximum efficiency and optimal flow rate for the turbine can be achieved. Figure 3 shows the flowchart of the genetic algorithm for optimizing efficiency for the flow rate parameter.

### 4. Numerical Study

Due to the fact that the experimental tests device of the Archimedes screw turbine does not have the ability to check the turbine in the optimal flow rate, the performance characteristics of the turbine at the optimal flow rate are investigated using the numerical simulation. Star CCM+ software is used for this purpose. This software is one of the most powerful software for simulation and analysis of physical problems. In the numerical study, first, turbine simulated a flow rate of 2.4 (lit/s), which is the closest to the optimal flow rate. After validating the simulation results in this flow rate with the experimental results, the numerical simulation results for this and the optimal flow rate are compared.

#### 4.1 The physics of the problem

As mentioned, Fig. 2 shows the experimental test device. According to this form, the physics of the problem will consist of two sections that have different movement systems. The first section, which includes the turbine and has a rotating motion system, is called the rotational section in the simulation. The second part is the input flow to the turbine, which has a linear motion system and is known as the non-rotational section in the simulation. In this section of the paper, creating the simulation geometry and determining the motion system for different parts of the simulation geometry are determined.

##### 4.1.1 Simulation geometry

The Archimedes screw turbine model is designed in SolidWorks software and then imported into Star CCM+ software for numerical simulation. The model imported in the software is placed in a cylindrical domain, which determines the turbine meshes' location. This domain has a slightly larger diameter and length than the diameter and length of the turbine. This cylinder and turbine are classified as the rotational section of the simulation. Next, this section will be placed inside a larger cylindrical domain, which will actually be the main tank for the input and output of the flow. This large cylinder, which has larger dimensions than the turbine, is classified with another cylinder with the dimensions of a small cylinder around the turbine, in the non-rotational section of the simulation. In the following, these two equal-sized cylinders are used in the rotational and non-rotational sections of the simulation to create an interface. The dimensions of the created cylinders are determined according to the proposal of Javanmard et al. [33]. Figure 4 shows rotational and non-rotational sections and their dimensions.

##### 4.1.2 Motion models

As mentioned, two motion systems are needed for this simulation. For the non-rotational section of the simulation, which is related to the inlet and outlet of the flow, the Cartesian motion system is determined according to the software's default settings. The MRF method is used for the motion system of the simulation's rotational section. MRF is a method for solving rotating systems problems. Using this method, the turbine's rotational speed in different conditions is used as the input of the simulation software. The turbine rotates with certain rotational speeds and the performance characteristics of the turbine are checked when the flow enters the turbine. Figure 4 shows the turbine simulation geometry and its different sections.

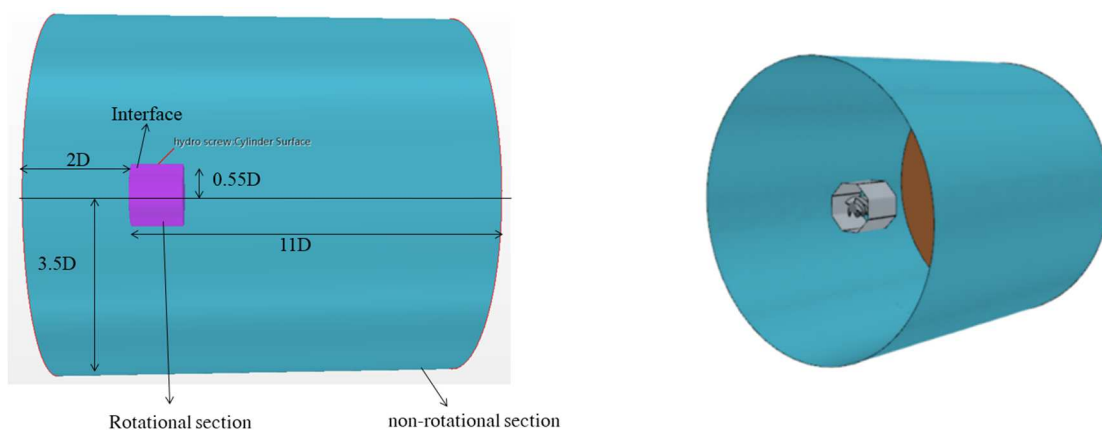


Fig. 4. Simulation geometry of Archimedes screw turbine and its different sections and their dimensions (D: Turbine outer diameter).



4.2 Governing equations of simulation

Equation 7 shows the continuity equation [17]:

$$\frac{\partial(u)}{\partial x} + \frac{\partial(v)}{\partial y} + \frac{\partial(w)}{\partial z} = 0 \tag{7}$$

This equation is used to calculate mass conservation. This equation uses the variables of density, time and different directions and velocities related to these directions. In the following, the momentum equation is examined [13]:

$$\rho(u \frac{\partial u}{\partial x} + v \frac{\partial u}{\partial y} + w \frac{\partial u}{\partial z}) = -\frac{\partial P}{\partial x} + \rho g_x + \mu(\frac{\partial^2 u}{\partial x^2} + \frac{\partial^2 u}{\partial y^2} + \frac{\partial^2 u}{\partial z^2}) \tag{8}$$

$$\rho(u \frac{\partial v}{\partial x} + v \frac{\partial v}{\partial y} + w \frac{\partial v}{\partial z}) = -\frac{\partial P}{\partial y} + \rho g_y + \mu(\frac{\partial^2 v}{\partial x^2} + \frac{\partial^2 v}{\partial y^2} + \frac{\partial^2 v}{\partial z^2}) \tag{9}$$

$$\rho(u \frac{\partial w}{\partial x} + v \frac{\partial w}{\partial y} + w \frac{\partial w}{\partial z}) = -\frac{\partial P}{\partial z} + \rho g_z + \mu(\frac{\partial^2 w}{\partial x^2} + \frac{\partial^2 w}{\partial y^2} + \frac{\partial^2 w}{\partial z^2}) \tag{10}$$

Equation (11) is used as RANS equation in x direction for solving Navier-Stokes equations [13]:

$$\rho \left[ \frac{\partial}{\partial x}(\overline{u^2}) + \frac{\partial}{\partial y}(\overline{uv}) + \frac{\partial}{\partial z}(\overline{uw}) \right] = -\frac{\partial \overline{p}}{\partial x} + \frac{\partial}{\partial x}(\mu \frac{\partial \overline{u}}{\partial x} - \rho \overline{u'u'}) + \frac{\partial}{\partial y}(\mu \frac{\partial \overline{u}}{\partial y} - \rho \overline{u'v'}) + \frac{\partial}{\partial z}(\mu \frac{\partial \overline{u}}{\partial z} - \rho \overline{u'w'}) \tag{11}$$

4.2.1 Turbulence model

A turbulence model closes the RANS system and makes it solvable. Because the SST k-omega turbulence model is an optimal state of k-epsilon (suitable for outside the boundary layer) and k-omega (suitable for inside the boundary layer) turbulence model, in this paper, according to physics of problem and geometry of simulation, on the one hand, it consists of many boundaries around the turbine, and on the other hand, it contains a large flow domain that is not affected by the boundary layer, the SST K-Omega turbulence model is used. Also, by studying similar studies in this field, it can be seen that this turbulence model is used in the simulations of this turbine [13, 14, 22]. This model consists of two equations, which include the turbulence kinetic energy equation (K) and the turbulence loss rate (omega), which are expressed according to equations (12) and (13) [34]. Equation (14) also shows the production of kinetic energy caused by turbulence shear stress:

$$u_i \frac{\partial \omega}{\partial x_i} = \frac{\omega}{k} P_r - \beta \omega^2 + \frac{\partial}{\partial x_i} \left[ (\mu + \sigma_\omega \frac{k}{\omega}) \frac{\partial \omega}{\partial x_j} \right] + \frac{\sigma_d}{\omega} \frac{\partial k}{\partial x_j} \frac{\partial \omega}{\partial x_j} \tag{12}$$

$$u_i \frac{\partial \omega}{\partial x_i} = P_r - \beta^* \omega k + \frac{\partial}{\partial x_j} \left[ (\mu + \sigma_k \frac{k}{\omega}) \frac{\partial k}{\partial x_j} \right] \tag{13}$$

$$P_r = \tau_{i,j} \frac{\partial u_i}{\partial x_j} \tag{14}$$

4.2.2 Volume friction

Since two fluid types are used in the simulation of the Archimedes screw turbine, this paper will use the VOF method to define the free surface and control the volume [35]:

$$u_j \frac{\partial f_i}{\partial x_j} = 0 \tag{15}$$

Considering that the sum of the phases is equal to 1 and the fluid volume is constant. that's mean [35]:

$$\sum_{m=1}^n f_m = 1 \tag{16}$$

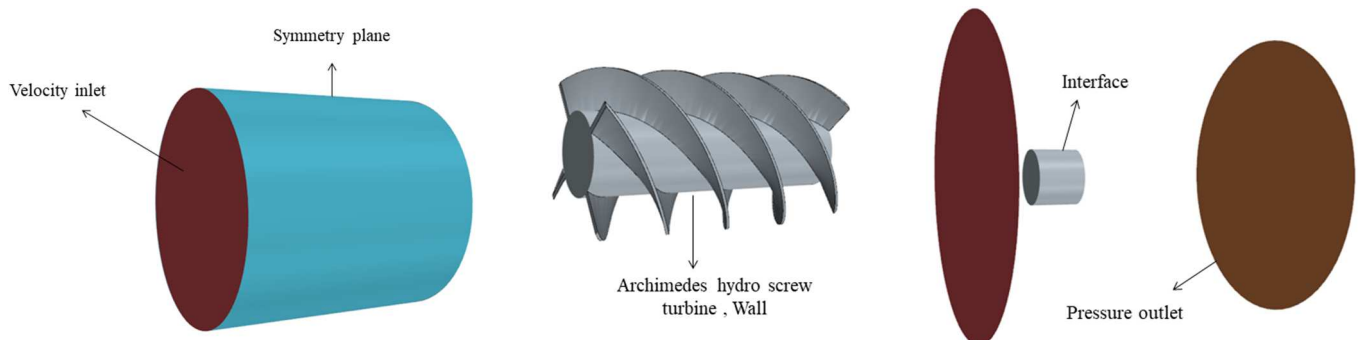


Fig. 5. Boundary conditions of different parts of simulation geometry.



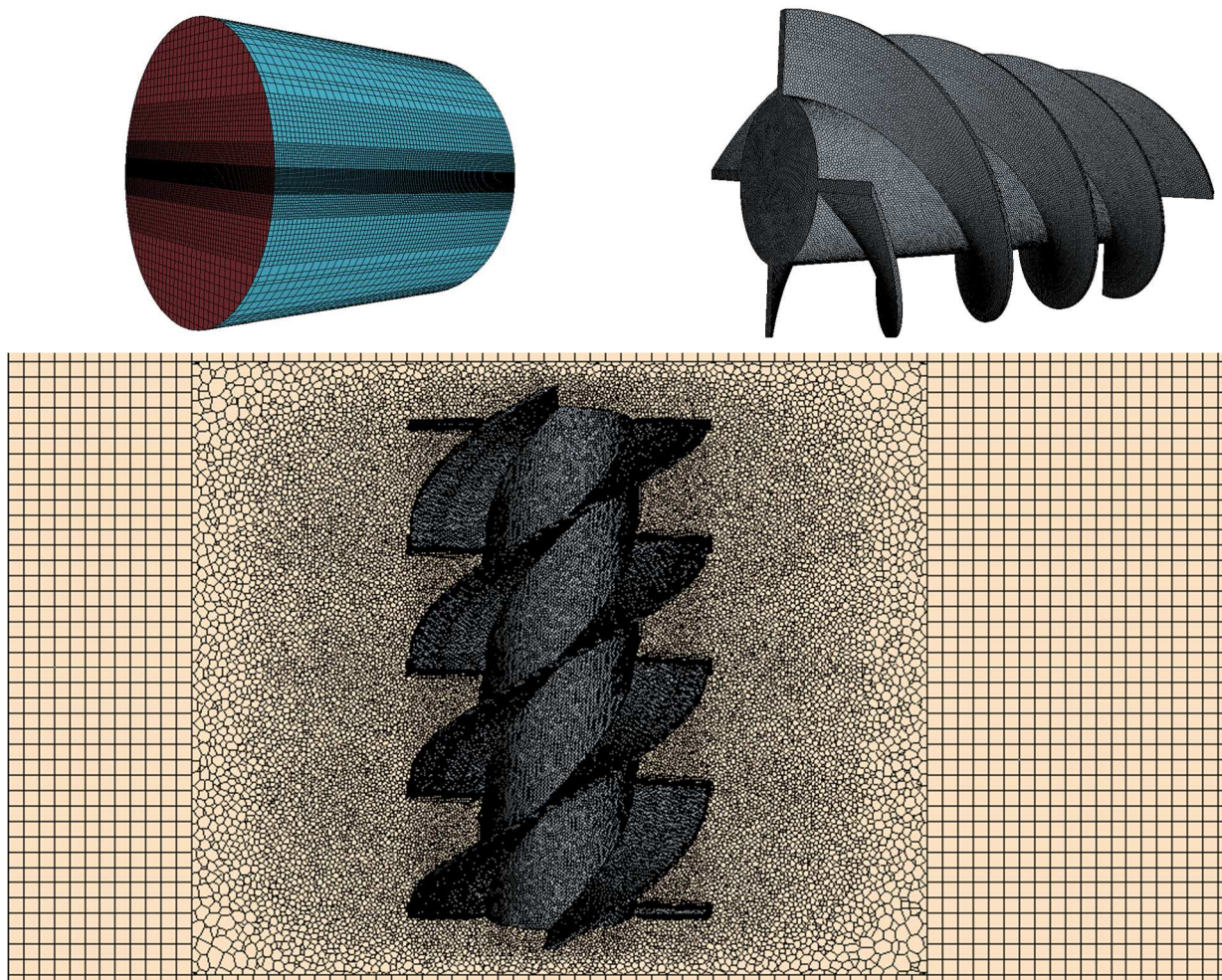


Fig. 6. Meshing of Archimedes screw turbine simulation.

#### 4.3 Boundary condition

Considering that all region of simulation is in wall condition by default and the boundary layer meshes is created near the walls, therefore, before creating the mesh, the type of boundaries is determined. Velocity inlet condition is selected for the flow tank inlet, pressure outlet condition is selected for the tank outlet plate, and symmetry plane condition is selected for the plates around the tank cylinder. Since in the simulation with multiple regions in the Star CCM+ software, while the mass and energy values are transferred between the regions during the calculations, Interface boundary conditions are used. In this simulation, it is necessary to create an interface between the rotational and non-rotational sections. The small cylinders of these sections, which will be the interface, are first placed in the wall condition. After being combined, they are saved as the interface in the software settings. According to the use of the MRF motion model in the simulation, the screw turbine also has a wall condition.

#### 4.4 Meshing of simulation

In this stage of simulation, which is actually one of the most important stages, a suitable mesh for simulation should be created according to the geometry and physical conditions of different parts. Since the general geometry in this simulation is divided into rotational and non-rotational sections and the rotational section is more important in the simulation (because of the presence of turbine in this section), two separate meshes are created for each of these two sections. Also, since the free surface of the flow is essential, a separate control mesh is created for it. For meshing for the rotational section of the geometry, surface meshes, polyhedral meshes, and prism layer mesh models are used. The surface meshes and trimmer models are used for the non-rotational section, which is less important in the simulation. To check the boundary layer meshes, the boundary layer mesh is created by calculating the first created boundary layer, the total thickness, and the number of boundary layers. According to the simulations of the semi-submerged propeller, equation (17) calculates the first created boundary layer [33]:

$$\Delta y = 8.6Ly^+ Re^{-\frac{13}{14}} \quad (17)$$

Another important issue in numerical simulations is investigating the effect of the grid size on the final result of the simulation. Therefore, it is necessary to evaluate the results' independence from the simulation's grid size. The goal of an independent solution from the grid is to achieve the largest meshes that can simulate the desired function with the desired accuracy. Figure 7 shows the result of checking the independence from the grid for the power parameter for this simulation for the flow rate of 2.4 (lit/s) and electrical resistance of 10 (Ohm). The different values of the number of grids have been specified according to the standards in the software settings and according to the recommendation of Ebrahimi et al. [36]. According to this figure, the number of grids for this simulation is equal to 5132905, of which 4109048 are related to the rotational section and the rest are related to the non-rotational section of the simulation.



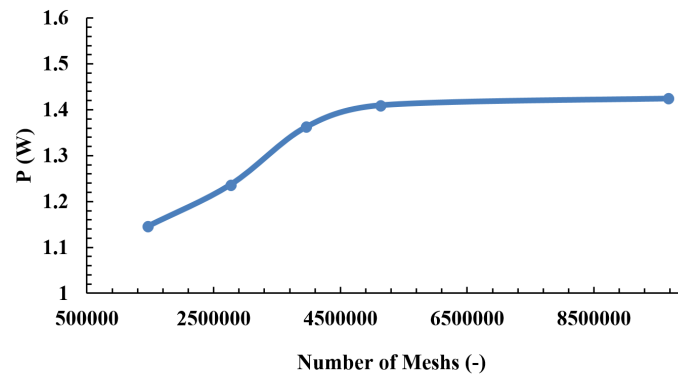


Fig. 7. Checking the independence of the grid for the power parameter in the numerical simulation of the Archimedes screw turbine.

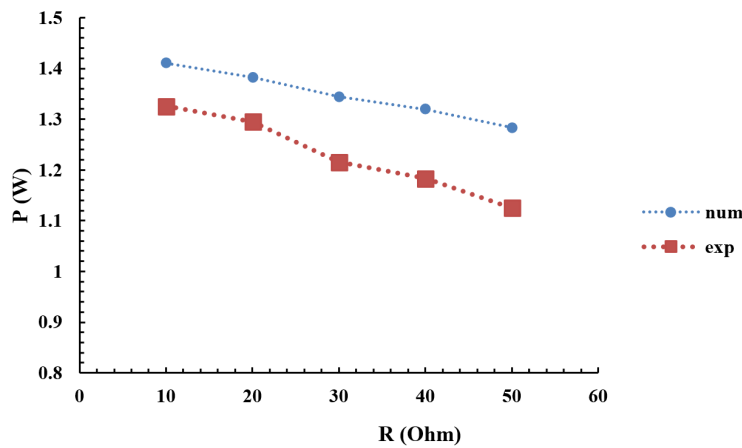


Fig. 8. The diagram related to the validation of the results of experimental tests and numerical simulation for power according to electrical resistance at the flow rate of 2.4 (lit/s).

4.5 Validation of experimental and numerical results

After completing the various stages of experimental tests and numerical simulation, in order to validate these methods, a comparison between the results of experimental tests and numerical simulation is made in this section. This validation is evaluated for the 2.4 (lit/s) flow rate, which is the closest flow rate to the optimal flow rate. Figure 8 shows the diagram related to the changes in the output power of the turbine according to electrical resistance for the flow rate of 2.4 (lit/s) for both experimental and numerical results. The values of the output power in these two conditions and the errors related to it are shown in Table 2 for validation.

At the end of this section, Table 3 is used to specify the range of different parameters to perform numerical simulations of Archimedes screw turbine in the StarCCM+ software.

5. The Economic Study of Archimedes Screw Turbine Hydropower Plant

The performance of the Archimedes screw turbine in the prototype scale of this turbine (which is 6 times the size of the laboratory model) studied by using Froude scaling [24]. Considering that the cost of building a hydroelectric power plant is calculated according to equation (18) [37] and the global price of electricity is equal to 0.13 \$/kWh [38], it is possible to study the construction and operation of the turbine in the prototype scale from an economic point of view:

$$\text{construction cost (\$)} = 0.27 \times \text{Annual production electricity (KWh)} \tag{18}$$

Table 2. Validation of the results of experimental measurements and numerical simulation according to electrical resistance at the flow rate of 2.4 (lit/s).

Electrical resistance (Ohm)	The output power of experimental tests (W)	The output power of numerical simulation (W)	Relative error (%)	Mean error (%)
10	1.3255	1.4102	6.41	
20	1.3045	1.3826	6.01	
30	1.2157	1.3442	10.56	9.68
40	1.1838	1.3194	11.45	
50	1.1255	1.2831	14.01	

Table 3. Ranges of utilized parameter for simulation of Archimedes screw turbine.

Parameter	Flow rate (lit/s)	Electrical Resistance (Ohm)	Rotational speed (rpm)
Range of changes	2.4, 2.6	10-50	220-238



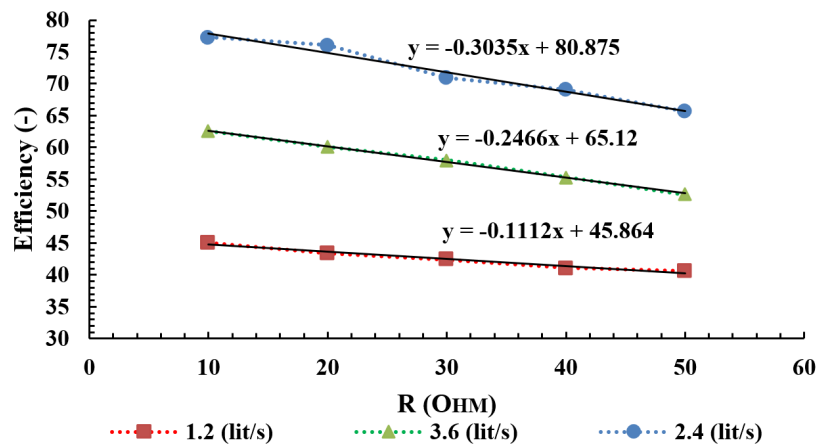


Fig. 9. The diagram of changes in turbine efficiency according to the electrical resistance in different flow rate according to experimental tests [24].

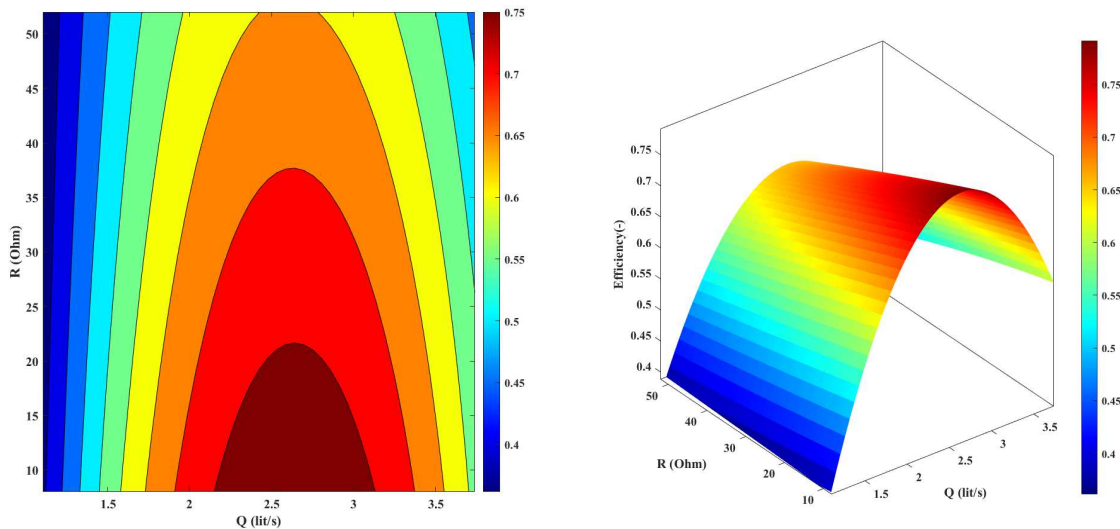


Fig. 10. 3D counter of turbine efficiency according to flow rate and electrical resistance.

The Discounted Payback Period (DPP) is the investment return period according to the annual discount rate and is calculated according to equation (19) [39, 40]:

$$DPP = \frac{-\ln\left(1 - \frac{Inu * Disc}{CF}\right)}{\ln(1 + Disc)} \tag{19}$$

Also, according to the cost of building a hydroelectric power plant in Iran [24], the issue of saving currency can be studied.

## 6. Results

### 6.1 The results of the experimental study

According to the device for conducting experimental and design of experiment, the effect of the changes in the input flow rate to the turbine in different states of the rheostat electrical resistance on the performance characteristics of the turbine has been investigated. The results showed that with the increase of the rheostat resistance at a constant flow rate, the values of rotational speed, torque, output power, and efficiency of the turbine decrease. Also, with the increase of the input flow rate to the turbine, the rotational speed, torque and output power always increase, and the efficiency of the turbine first increases with the increase of the flow rate. After reaching its maximum value, it begins to decrease with the flow rate increase. First, the increase in turbine efficiency is due to the increase in turbine output power. Further, with the increase in turbine flow rate, the rotational speed of the turbine exceeds the maximum speed limit for this turbine and reduces the efficiency of the turbine due to the increase in the flow turbulence. Figure 9 shows the diagram of turbine efficiency changes based on experimental tests. This figure clearly shows that the highest turbine efficiency values occur for the flow rate of 2.4 (lit/s).

### 6.2 Optimization of experimental results

The aim of optimizing the results of experimental tests is to reach the maximum achievable efficiency for the Archimedes screw turbine. Figure 10 shows the three-dimensional diagram related to the changes in turbine efficiency according to the results of experimental tests. As mentioned, the highest efficiency value in experimental tests happened at 2.4 (lit/s) flow rate. But according to this figure, it is clear that the turbine's efficiency increases for a while after this flow rate and reaches its maximum value. Therefore, it is possible to calculate the maximum accessible efficiency value and the flow rate related to this efficiency value by using Genetic Algorithm optimization for Archimedes screw turbine.



**Table 4.** The maximum value of turbine efficiency for different flow rates.

Flow rates (lit/s)	Maximum turbine efficiency (%)
1.2	45.1
2.4	77.2
2.6	78.5
3.6	62.6

**Table 5.** Values of rotational speed in optimal flow rate.

Electrical resistance (Ohm)	10	20	30	40	50
Rotational speed at optimal flow rate (rpm)	238	236	233	231	228
Maximum error (%)	0.2				

For this purpose, using equation (20), which is the equation of curve fitting (of figure 10) and obtained using the CFTool MATLAB software toolbox, this optimal flow rate can be calculated for the turbine. According to the experimental tests and also the efficiency equation, the maximum efficiency for the Archimedes screw turbine occurs when the rheostat resistance is at its lowest value, i.e., at 10 (Ohm):

$$f(Q,R) = -0.4143 + 0.931Q + 0.002982R - 0.1764Q^2 - 0.004583QR + 1.124e^{-5}R^2 + 0.0008971Q^2R + 6.161e^{-6}R^2Q + 1.667e^{-8}R^3 \quad (20)$$

According to Fig. 11, to optimize the efficiency results of the Archimedes screw turbine, equation (20) is used in the optimization toolbar of MATLAB software to find the best fitness. The 2.6 (lit/s) flow rate is determined as the optimal value for the turbine.

**6.3 The results of numerical study**

In this section, the results of the numerical simulation for the flow rate of 2.4 (lit/s) and the optimal flow rate (2.6 (lit/s)) are compared in the form of different diagrams and contours.

**6.3.1 The results of turbine performance**

Considering the creation of a rotational reference frame for turbine simulation, the rotational speeds obtained from experimental tests should be used as input for the rotational reference frame's rotational speed value. For the flow rate of 2.4 (lit/s), the rotational speeds obtained from the experimental tests are available. However, the rotational speed diagram of experimental tests should be used for optimal flow rate. Figure 11 shows the three-dimensional diagram of rotational speed changes for the turbine according to the results of experimental tests. To calculate the turbine's rotational speed in the optimal flow rate, equation (21) is used, which is the equation of the fitting curve of the diagram in Figure 12. By putting the optimal flow rate and different values of rheostat resistance in this equation, the rotational speeds at the optimal flow rate are calculated with a maximum error of 0.2%.

$$h(Q,R) = 25.65 + 129.9Q - 0.1218R - 18.39Q^2 - 0.05422QR - 2.193e^{-17}R^2 \quad (21)$$

Table 6 shows the rotational speed values for the optimal flow rate. The maximum error of 0.2% specified in this table is presented by inserting different values of the electrical resistance for flow rate of 2.4 (lit/s) in equation (21) and comparing the results with the results of experimental tests.

The rotational speeds obtained in this section are used as software inputs to simulate the turbine in the optimal flow rate. Figure 12 shows the diagram of rotational speed changes according to different electrical resistances for two flow rates of 2.4 and 2.6 (lit/s). According to this figure, the rotational speed in optimal flow rate is higher than the flow rate of 2.4 (lit/s). Because by increasing the input flow rate to the turbine, the momentum value increases at the optimal flow rate. Also, according to this figure, for both flow rates, similar to the results of experimental tests, with the increase in electrical resistance, the turbine's rotational speed decreases. The rate of rotational speed reduction in both cases is almost equal. The rotational speeds obtained for the optimal flow, compared to other flow rates, have the least difference compared to the rotational speed limit. This is another reason for the optimal performance of the turbine (maximum efficiency) in this flow rate.

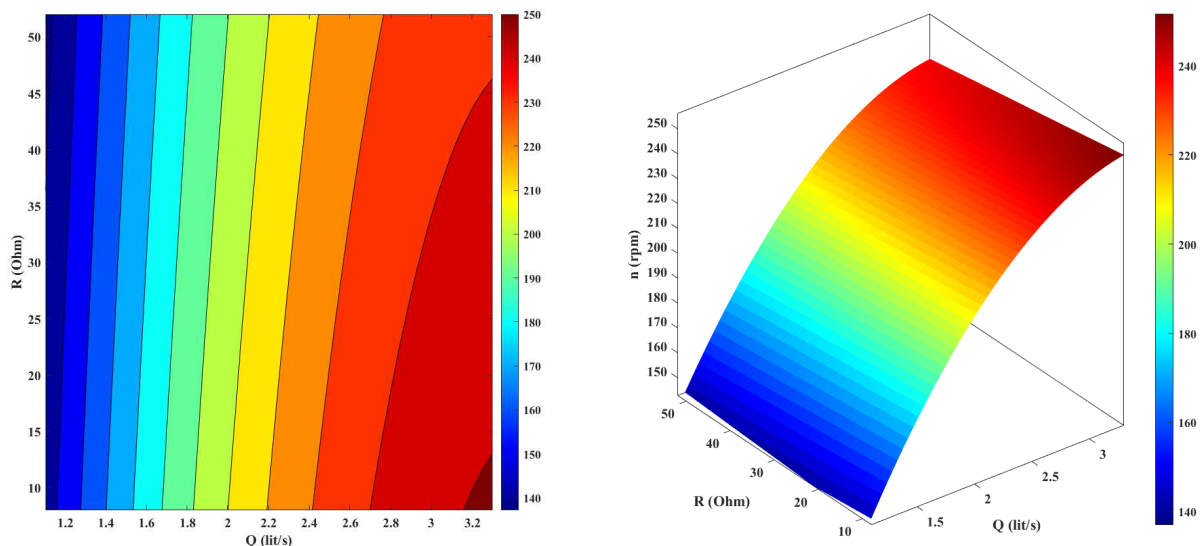


**Fig. 11.** 3D diagram of rotational speed changes according to the input flow to the turbine for different electrical resistances.



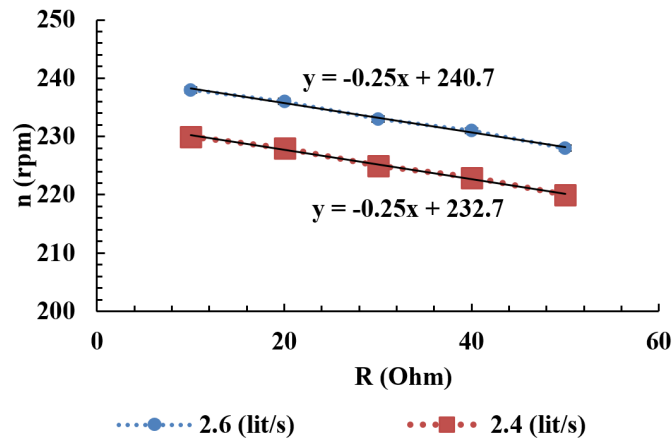


Fig. 12. Rotational speed of turbine according to electrical resistance for flow rates of 2.4 and 2.6 (lit/s).

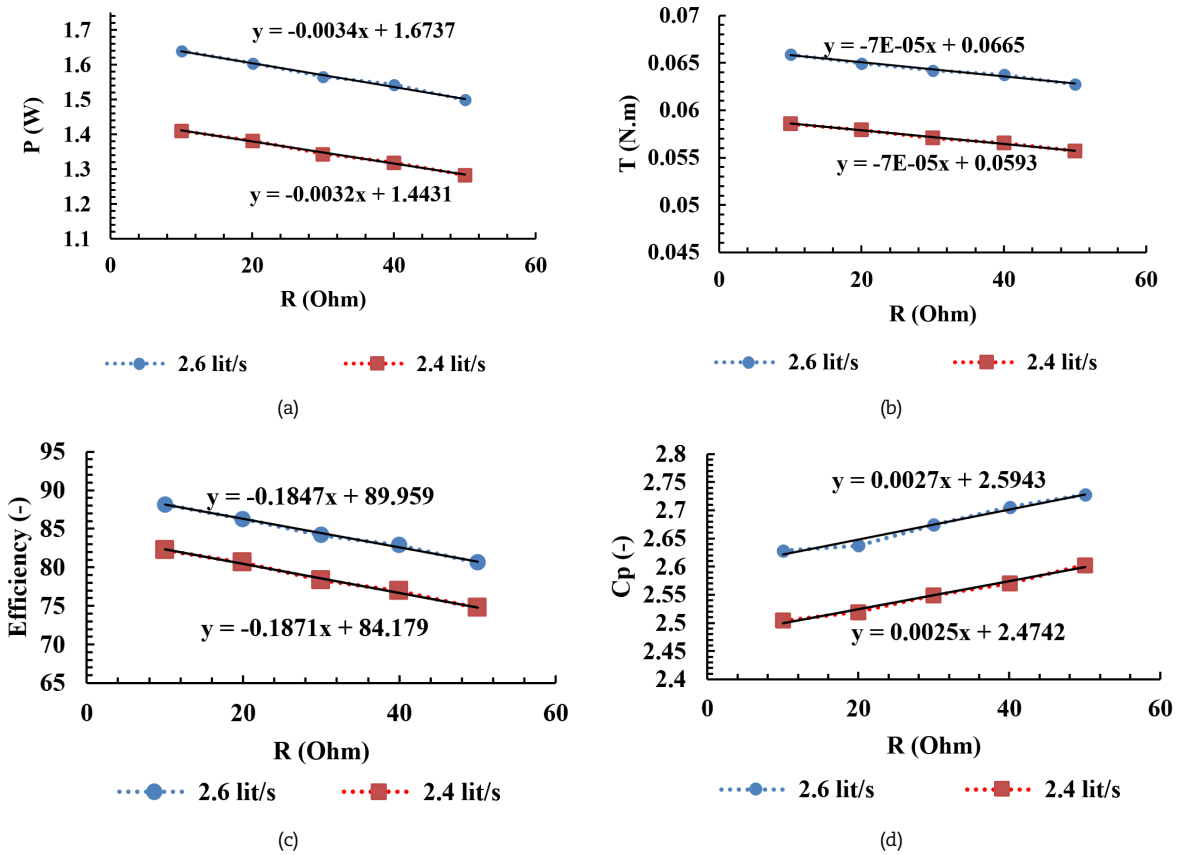


Fig. 13. Diagram of changes in a) power, b) torque, c) efficiency and d) power coefficient resulting from the numerical simulation of the turbine according to electrical resistance changes for flow rates of 2.4 and 2.6 (lit/s).

Figure 13 (a) to (d) shows the diagrams of power, torque, efficiency and power coefficient changes obtained from the numerical simulation of the Archimedes screw turbine according to electrical resistance changes for two flow rates of 2.4 and 2.6 (lit/s). According to Figure 13 (a), the output power values of the turbine for different states of electrical resistance in the optimal flow rate are higher than the flow rate of 2.4 (lit/s). As it was found in the results of the experimental tests, according to the turbine power equation, the turbine's output power increases with the flow rate increase in constant electric resistance. This is why the output power is higher in the optimal flow rate in Figure 13 (a). Also, according to this figure, it is clear that the output power of the turbine decreases with the increase of electrical resistance. The power reduction rate with the change of electrical resistance for the optimal flow rate is about 5 % higher than the 2.4 (lit/s) flow rate. Also, according to this figure, the sensitivity of output power changes to changes in electric resistance (consumed load) in the diagram obtained from numerical simulation is less than the diagram obtained from experimental results.

Figure 13 (b) shows the torque changes for these two flow rates according to electrical resistance changes. The process of changes in this diagram is the same as the process of changes in the power diagram and the torque values in the optimal flow rate have increased compared to the flow rate of 2.4 (lit/s). In both cases, the torque values decrease with increased electrical resistance. The sensitivity of torque to electrical resistance in these two flow rates is almost the same, but it has decreased compared to the results of experimental tests. Figure 13 (c) shows the diagram of the changes in the efficiency of the Archimedes screw turbine resulting from the numerical simulation of the turbine according to changes in electrical resistance for these two flow rates. Since optimizing the performance of the turbine is to achieve the highest possible efficiency, the turbine efficiency values will have the highest values at the optimal flow rate. The process of changes in efficiency is the same as the process of



changes in the power and torque diagram. The increase in flow rate, which has resulted in the increase in output power, according to the turbine efficiency equation, increases. With the increase in electrical resistance at a constant flow rate, it decreases due to the decrease in output power. Figure 13 (d) shows the diagram of changes in turbine power coefficient according to changes in electrical resistance for these two flow rates. This figure shows that the power coefficient values are higher in the optimal flow rate than the 2.4 (lit/s). It is also clear in this figure that with the increase of the electrical resistance, the value of the power coefficient increases with a constant flow rate. According to the power coefficient equation, the value of the power coefficient has a direct relationship with the output power from the turbine and an inverse relationship with the cube of the turbine's rotational speed. Due to the fact that with the increase of electrical resistance, the rotational speed and output power of the turbine decrease, Therefore, according to power coefficient equation, the rotational speed has a power of 3, and it is in the denominator of this equation, its reduction rate overcomes the power reduction rate. Finally, it causes an increase of the power coefficient. Also, due to the increase in electrical resistance, the rotational speed of the turbine decreases; therefore, according to the Reynolds number equation, this number also decreases for the turbine. According to the reduction of the dimensionless Reynolds number, the values of power coefficient of turbine increase. This process was previously shown in the experimental results [24] of the power coefficient of the Archimedes screw turbine.

6.3.2 The results of simulation contours

After presenting the diagrams related to the performance characteristics obtained from the numerical simulation of the turbine, this section shows the behavior of the Archimedes screw turbine in the optimal flow rate and the flow rate of 2.4 (lit/s) is evaluated using different contours obtained from numerical simulation. Figure 14 shows the vorticity contour for the turbine's two input flow rates. According to this figure, the vorticity values for the Archimedes screw turbine at a flow rate of 2.4 (lit/s) are higher than at a flow rate of 2.6 (lit/s). Higher vorticity values indicate higher vortical flow in the flow rate of 2.4 (lit/s), which causes more energy to be wasted in this flow rate compared to the optimal flow rate. This figure shows the better performance of the turbine and less energy loss in the optimal flow rate, which will result in higher efficiency in this optimal flow rate.

Figure 16 shows the pressure contour for these two flow rates. According to this figure, the pressure values in the optimal flow rate are higher than the 2.4 (lit/s) flow rate. Considering that the optimal flow rate is higher than the flow rate of 2.4 (lit/s), this increase in flow rate and pressure together, increase the power in this flow rate. Also, according to this figure, the pressure contour in the optimal flow rate is more continuous compared to the flow rate of 2.4 (lit/s), which causes less power loss in the optimal flow rate.

Figure 16 shows the velocity contour for these flow rates. According to this figure, the process of velocity changes in different parts of the Archimedes screw turbine is almost the same for two flow rates. But the velocity values in the optimal flow rate are higher than the flow rate of 2.4 (lit/s). This increase in velocity is due to the increase in flow rate. This increase in velocity and pressure shown in Figure 15 for this flow rate will increase the power in the optimal flow rate and will have fewer losses in this flow rate.

Figure 17 also shows the phase contour for the turbine's two input flow rates. Due to the fact that in the simulation of the Archimedes screw turbine two fluids, water and air, are used, to show the phase changes on the Archimedes screw turbine, the density of these two materials is used as the phase contour. In some screw turbines, immersion leakage occurs at the exit of the screw and the water does not come out completely from the outlet of the screw and in fact, the bucket at the end of the screw is removed or made smaller by the water, and the length of screw becomes lower. This immersion reduces the turbine's efficiency [27, 12, 3]. According to Figure 17 and comparing the state of the water and air phase at the exit of the screw, it is clear that in the optimal flow rate compared to the flow rate of 2.4 (lit/s), the amount of water in the turbine outlet is less and its discharge is better and its immersion is less. Also, in this figure, the increase in the amount of water at the turbine inlet for the optimal flow rate is clear. Therefore, it can be concluded that the performance of the turbine in the flow rate of 2.6 (lit/s) is better compared to 2.4 (lit/s) and the losses are fewer in this optimal flow rate.

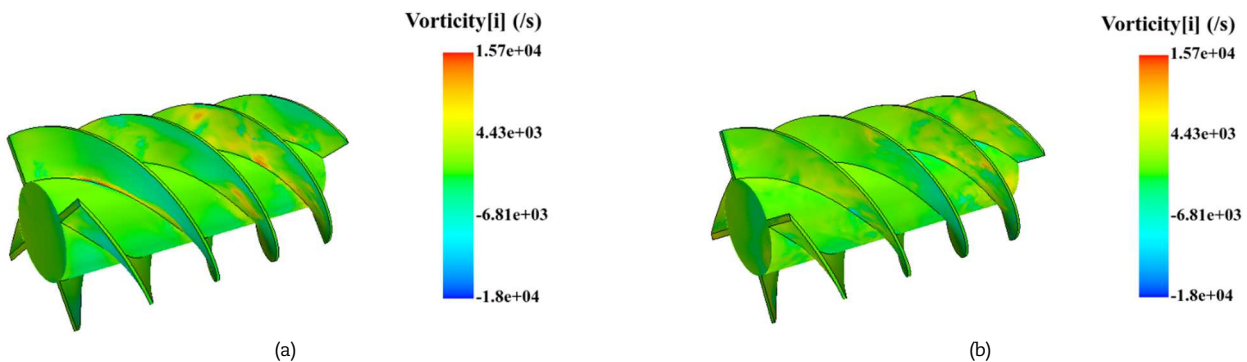


Fig. 14. Turbine Vorticity contour at flow rates a) 2.4 and b) 2.6 (lit/s).

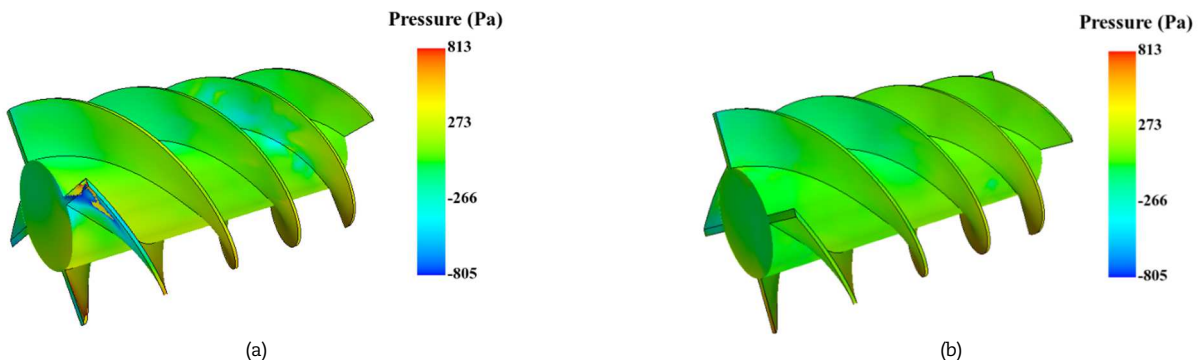


Fig. 15. Turbine pressure contour at flow rates a) 2.4 and b) 2.6 (lit/s).



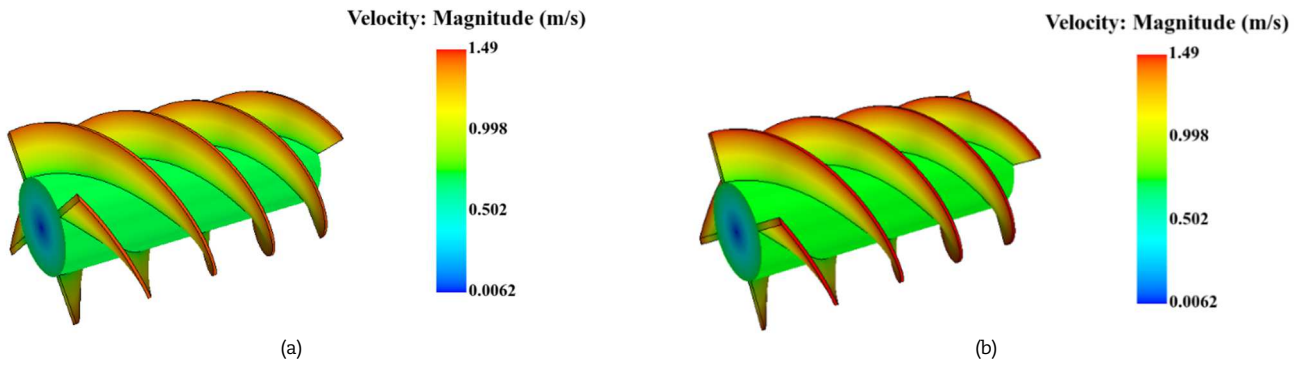


Fig. 16. Turbine velocity contour at flow rates a) 2.4 and b) 2.6 (lit/s).

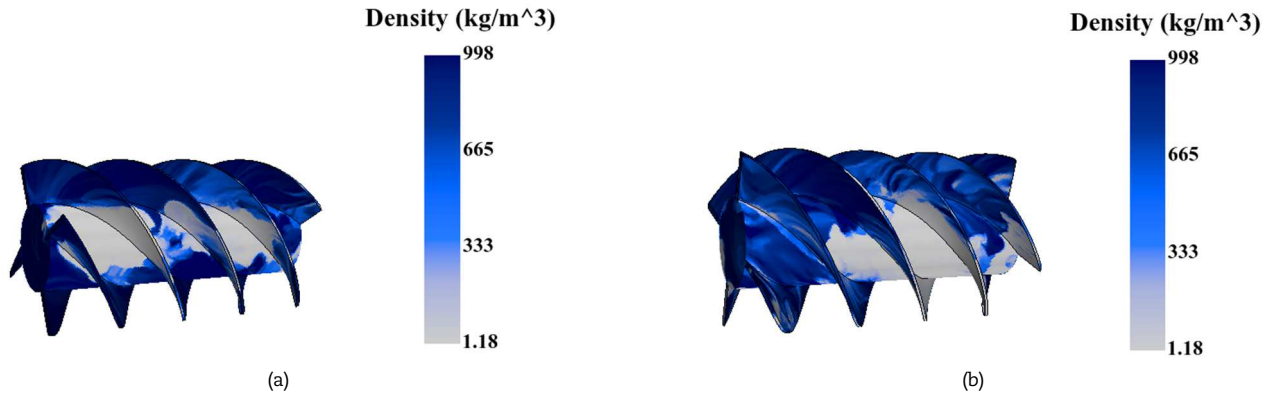


Fig. 17. Turbine phase contour at flow rates a) 2.4 and b) 2.6 (lit/s).

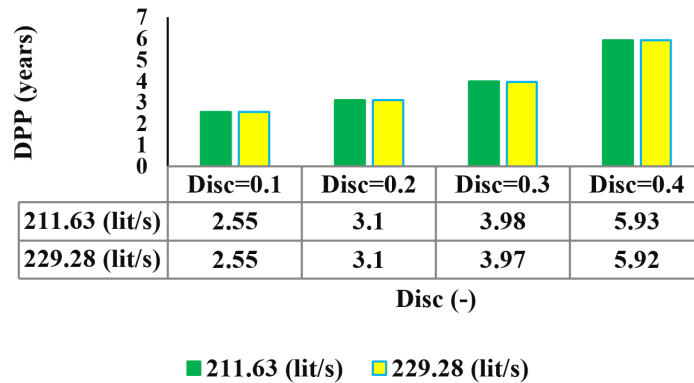


Fig. 18. Discount payback period according to discount rate.

### 6.4 The results of economic study

In this section, according to the validation mentioned above, the output powers obtained from the numerical simulations for two flow rates of 2.4 and 2.6 (lit/s) are determined for the experimental condition. In the following, these powers are generalized using by Froude scaling for the turbine in the prototype scale (6 times of the laboratory model). So that by using these results, the construction and operation of the Archimedes screw turbine on the prototype scale as a hydroelectric power plant will be analyzed economically. Table 6 shows the amount of annual electricity production, costs, and income related to the turbine operation for these two flow rates on a prototype scale.

To calculate the DPP, taking into account the different discount rates in different countries and also examining similar studies [26], this parameter is evaluated for 4 discount rate scenarios of 0.1, 0.2, 0.3, and 0.4. Figure 18 shows the discount payback period according discount rate for these two flow rates. According to this figure, the discount payback period increases with the increase in the discount rate. Also, it is clear in this figure that flow rate does not have much effect on the discount payback period and this parameter varies between 2.55 and 5.93 years for both flow rates according to the discount rate. After this period, the turbine enters the profitability stage and according to the annual electricity sales price in table 6, it will be capable of making a profit of 886 (\$) (in optimal flow rate conditions).

Table 6. The results of economic study of prototype turbine.

Flow rate (lit/s)	Annual electricity production (kWh)	Power plant construction cost (\$)	Power plant maintenance cost (\$)	Total costs (\$)	Annual income from selling electricity (\$)
211.63	6143.47	1658	66	1724	798
229.28	6662.51	1799	71	1870	866



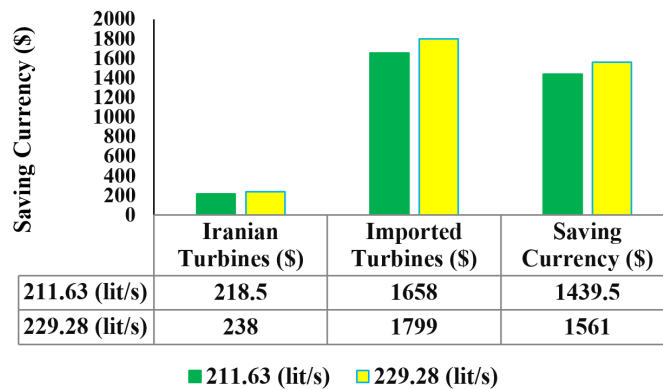


Fig. 19. Amounts of costs related to the construction of the Archimedes screw turbine power plant in Iran and the foreign model and the amount of currency savings.

Figure 19 shows the diagram of changes in cost according to the input flow rate to the Archimedes screw turbine for the Iranian and foreign models. The amount of currency savings by using the Iranian model is also shown in this diagram. According to this figure, the cost values of the Iranian and the imported model and as a result, the currency savings are higher for flow rate of 229.28 (lit/s) (optimal flow rate in prototype scale) and the use of the turbine at the optimal flow rate in the prototype scale can save currency by 1561 (\$).

## 7. Conclusion

In this paper, after a short review of the experimental study of Archimedes screw turbine and its results, the optimization of these results was done by using the genetic algorithm method with the aim of achieving the maximum efficiency of the turbine. Due to the impossibility of conducting experimental tests at the optimal flow rate, the performance characteristics of the turbine at this flow rate were determined by numerical simulation of the turbine in the Star CCM+ software and the performance of the turbine at this flow rate and the closest flow rate, whose experimental results were also available, were compared. In the following, the construction and operation of the turbine in the prototype scale as a hydroelectric power plant was evaluated economically. The general results obtained from this paper are as follows:

- In the experimental study, with the increase of the input flow rate to the turbine, the rotational speed, output power and torque values have always been on an upward trend. However, the turbine efficiency increases at first, and after reaching a maximum value, it starts to decrease. This is the basis for optimizing the experimental results to achieve the maximum efficiency of the turbine.
- After achieving the flow rate of 2.6 (lit/s) as the optimal flow rate, the comparison between the performance characteristics of the turbine at this flow rate and flow rate of 2.4 (lit/s) shows the increase in rotational speed, output power, torque, efficiency and power coefficient at this flow rate.
- By increasing the value of electrical resistance for optimal flow rate and flow rate of 2.4 (lit/s), the rotational speed, torque, output power and efficiency values decrease and the power coefficient values increase.
- The comparison of vorticity values in the optimal flow rate and the flow rate of 2.4 (lit/s) shows that the vortex currents are more in the flow rate of 2.4 (lit/s) and as a result more energy losses in this flow rate, which confirms the optimal performance of the turbine in the flow rate of 2.6 (lit/s).
- The comparison of velocity and pressure in these flow rates also shows that the changes of these values are greater and more uniform for the optimal flow rate, which indicates less power loss in this flow rate.
- The phase changes in the numerical simulation also show that there is more immersion at the end of the turbine outlet in the flow rate of 2.4 (lit/s), which can affect the turbine's performance and reduce the efficiency compared to the optimal flow rate.
- According to the economic study of the turbine in the prototype scale, the discounted payback period for optimal flow rate varies between 2.55 and 5.93 years according to the discount rate.
- The construction and operation of the turbine in the prototype scale as a hydroelectric power plant has the ability to save currency in the amount of 1561 (\$).

## Author Contributions

M. Zamani: Experimental Study, Numerical study, Writing, Data Analysis, discussion; R. Shafaghat: Supervisor, Design and construction, Design of Experiment. B. Alizadeh Kharkeshi: Methodology, Uncertainty Analysis, Reviewing, Editing.

## Acknowledgments

Not applicable.

## Conflict of Interest

The authors declared no potential conflicts of interest concerning the research, authorship, and publication of this article.



## Funding

The authors received no financial support for the research, authorship, and publication of this article.

## Data Availability Statements

The datasets generated and/or analyzed during the current study are available from the corresponding author on reasonable request.

## Nomenclature

CF	Cash flow in one year [\$]	n	Rotational speed of turbine [rpm]
$C_p$	Power coefficient [-]	P	Output power of turbine [W]
D	Diameter of turbine [m]	$P_{in}$	Input power [W]
DPP	Discount Payback Period [year]	$P_\tau$	Production of kinetic energy caused by turbulence shear stress [J]
Disc	Discount rate [-]	Q	Flow rate [lit/s]
$\Delta y$	Boundary layer thickness [m]	R	Electrical resistance [Ohm]
$\eta$	Efficiency [-]	Re	Reynolds number [-]
h	Head of turbine [m]	T	Torque [N.m]
I	Electric current [A]	V	Voltage [V]
Inv	Investment cost [\$]		
L	Characteristic length of the turbine [m]		

## Abbreviations

CFD	Computational Fluid Dynamics	RANS	Reynolds Average Navier-Stokes
DPP	Discount Payback Period	SST	Shear Stress Transport
MRF	Moving Reference Frame	VOF	Volume Of Fluid

## References

- [1] Abedanzadeh, A., Borgheipour, H., Fakouriyan, S., Torabi, F., Economic Evaluation of Supplying Commercial Thermal Load by a New CPVT System: A Case Study in Iran, *Journal of Applied and Computational Mechanics*, 9, 2023, 371-383.
- [2] Ceballos Zuluaga, J.M., Isaza Merino, C.A., Patiño Arcila, I.D., Morales Rojas, A.D., Fluid-dynamic Simulations for Assessment of Dimensioning Methodologies of Pelton Turbine Buckets Considering the Initial Torque Overcoming, *Journal of Applied and Computational Mechanics*, 2023, DOI: 10.22055/JACM.2023.42512.3935.
- [3] Kozyn, A., Lubitz, W.D., A power loss model for Archimedes screw generators, *Renewable Energy*, 108, 2017, 260-273.
- [4] Mohammadi, M., A.R., Mohammadi, M.R., Mohammadi, Optimizing Hydro Power Turbines in Order to Secure the Passage of Fishes in Khuzestan province, *Journal of Applied and Computational Mechanics*, 1, 2015, 95-102.
- [5] Rorres, C., The turn of the screw: Optimal design of an Archimedes screw, *Journal of Hydraulic Engineering*, 126, 2000, 72-80.
- [6] Schleicher, W.C., Numerical investigation and performance characteristic mapping of an Archimedean screw hydroturbine, Lehigh University, 2012.
- [7] Waters, S.R., *Analysing the performance of the Archimedes Screw Turbine within tidal range technologies*, Lancaster University, United Kingdom, 2015.
- [8] Lee, K.T., Kim, E.S., Chu, W.S., Ahn, S.H., Design and 3D printing of controllable-pitch archimedean screw for pico-hydropower generation, *Journal of Mechanical Science and Technology*, 29, 2015, 4851-4857.
- [9] Saroinsong, T., Soenoko, R., Wahyudi, S., Sasongko, M.N., Fluid Flow Phenomenon in a Three-Bladed Power-Generating Archimedes Screw Turbine, *Journal of Engineering Science & Technology Review*, 9, 2016, 72-79.
- [10] Lisicki, M., Lubitz, W., Taylor, G.W., Optimal design and operation of Archimedes screw turbines using Bayesian optimization, *Applied Energy*, 183, 2016, 1404-1417.
- [11] Songin, K., *Experimental analysis of Archimedes screw turbines*, University of Guelph, 2017.
- [12] Abdul Salam, C.A., Issac, J.M., Markose, B., NUMERICAL STUDY OF ARCHIMEDEAN SCREW TURBINE, *International Research Journal of Engineering and Technology*, 5, 2018, 2401-2405.
- [13] Simmons, S., *A computational fluid dynamic analysis of Archimedes screw generators*, University of Guelph, 2018.
- [14] Dellinger, G., Simmons, S., Lubitz, W.D., Garambois, P.A., Dellinger, N., Effect of slope and number of blades on Archimedes screw generator power output, *Renewable Energy*, 136, 2019, 896-908.
- [15] Montilla-López, A.I., Velásquez-García, L.I., Betancour, J., Rubio-Clemente, A., Chica-Arrieta, E.L., Performance of an Archimedes screw turbine with spiral configuration for hydrokinetic applications, *Revista Facultad de Ingeniería*, 2022, DOI: 10.17533/udea.redin.20221208.
- [16] Alonso-Martínez, M., Suárez Sierra, J.L., Coz Díaz, J.J.d., Martínez-Martínez, J.E., A new methodology to design sustainable archimedean screw turbines as green energy generators, *International Journal of Environmental Research and Public Health*, 17, 2020, 9236.
- [17] Stergiopoulou, A., Stergiopoulos, V., CFD Simulations of Tubular Archimedean Screw Turbines Harnessing the Small Hydropotential of Greek Watercourses, *International Journal of Energy and Environment*, 12, 2021, 19-30.
- [18] Lee, M.D., San Lee, P., Modelling the energy extraction from low-velocity stream water by small scale Archimedes screw turbine, *Journal of King Saud University-Engineering Sciences*, 2021, DOI: 10.1016/j.jksues.2021.04.006.
- [19] Shahverdi, K., Loni, R., Maestre, J., Najafi, G., CFD numerical simulation of Archimedes screw turbine with power output analysis, *Ocean Engineering*, 231, 2021, 108718.
- [20] Darmono, B., Pranoto, H., Archimedes Screw Turbines (ASTs) Performance Analysis using CFD Software Based on Variation of Blades Distance and Thread Number on The Pico Hydro Powerplant, *International Journal of Advanced Technology in Mechanical, Mechatronics and Materials*, 3, 2022, 18-25.
- [21] Zhang, D., Guo, P., Hu, Q., Li, J., Parametric study and multi-objective optimization of a ductless Archimedes screw hydrokinetic Turbine: Experimental and numerical investigation, *Energy Conversion and Management*, 273, 2022, 116423.
- [22] Adhikari, N., Adhikari, N., Poudel, S.K., Gurung, S., Subedi, S., Bastakoti, D., Study on Effect of Flow Rate and Number of Blades on Sizing of Archimedes Screw Turbine, IOE Graduate Conference, 2022.
- [23] Ubando, A.T., Marfori, I.A.V., Peradilla, M.S., Sy, C.L., Calapatia, A.M.A., Chen, W.H., Sustainable Manufacturability of Archimedes Screw Turbines: A Critical Review, *Journal of Manufacturing and Materials Processing*, 6, 2022, 161.
- [24] Zamani, M., Shafaghath, R., Kharkeshi, B.A., Experimental Investigation on the Effect of Flow Rate and Load on the Hydrodynamic Behavior and Performance of an Archimedes Screw Turbine, *International Journal of Engineering*, 36, 2023, 733-745.
- [25] Nugraha, A., Silalahi, D.S.H., Ansyah, P.R., Ramadhan, M.N., Amrullah, A., Cahyono, G.R., AN EXPERIMENTAL STUDY OF THE EFFECT OF VARIATION OF IMPACT LEVELS ON WORKING EFFICIENCY OF ARCHIMEDES SCREW TURBINE ON MICRO-HYDRO POWER PLANT, *International Journal of Mechanical Engineering Technologies and Applications*, 4, 2023, 1-9.
- [26] Ortiz Osornio, L.J., *Implementation and Usage of Low-cost Turbines for Power Generation in Water Networks*, Master's alternative plan paper, Minnesota State University, Mankato, USA, 2022.
- [27] Gogoi, P., Handique, M., Purkayastha, S., Newar, K., Potential of archimedes screw turbine in rural india electrification: a review, *ADBU Journal of*



*Electrical and Electronics Engineering*, 2, 2018, 30-35.

- [28] Lyons, M., Lubitz, W.D., *Archimedes screws for microhydro power generation*, ASME 2013 7th International Conference on Energy Sustainability collocated with the ASME 2013 Heat Transfer Summer Conference and the ASME 2013 11th International Conference on Fuel Cell Science, Engineering and Technology, 2013.
- [29] Stergiopoulou, A.V., Stergiopoulos, V.G., Tsioulos, D.I., Stylianou, A., *Two Innovative Experimental Archimedean Screw Energy Models In The Shadow Of Archimedes III*, in 5th International Conference on Experiments/Process/System Modeling/Simulation/Optimization, 2014.
- [30] White, F.M., *Fluid mechanics*, Tata McGraw-Hill Education, 1979.
- [31] Zamani, M., Shafaghat, R., Alizadeh Kharkeshi, B., *Experimental Investigation on the Effect of Flow Rate and Load on the Hydrodynamic Behavior and Performance of an Archimedes Screw Turbine*, *International Journal of Engineering*, 36, 2023, 733-745.
- [32] Kharkeshi, B.A., Shafaghat, R., Jahanian, O., Alamian, R., Rezanejad, K., *Experimental study on the performance of an oscillating water column by considering the interaction effects of optimal installation depth and dimensionless hydrodynamic coefficients for the Caspian Sea waves characteristics*, *Ocean Engineering*, 256, 2022, 111513.
- [33] Javanmard, E., Yari, E., Mehr, J.A., Mansoorzadeh, S., *Hydrodynamic characteristic curves and behavior of flow around a surface-piercing propeller using computational fluid dynamics based on FVM*, *Ocean Engineering*, 192, 2019, 106445.
- [34] Menter, F., *Zonal two equation kw turbulence models for aerodynamic flows*, in 23rd fluid dynamics, plasmadynamics, and lasers conference, 1993.
- [35] López, I., Pereiras, B., Castro, F., Iglesias, G., *Optimisation of turbine-induced damping for an OWC wave energy converter using a RANS-VOF numerical model*, *Applied Energy*, 127, 2014, 105-114.
- [36] Ebrahimi, A., Shafaghat, R., Hajiabadi, A., Yousefifard, M., *Numerical and Experimental Investigation of the Aero-Hydrodynamic Effect on the Behavior of a High-Speed Catamaran in Calm Water*, *Journal of Marine Science and Application*, 21, 2022, 56-70.
- [37] IRENA, W., *Hydropower*, IRENA Abu Dhabi, United Arab Emirates, 2012.
- [38] Sheykhi, M., Chahartaghi, M., Balakheli, M.M., Kharkeshi, B.A., Miri, S.M., *Energy, exergy, environmental, and economic modeling of combined cooling, heating and power system with Stirling engine and absorption chiller*, *Energy Conversion and Management*, 180, 2019, 183-195.
- [39] Bhandari, S.B., Iyer, R., *Predicting business failure using cash flow statement based measures*, *Managerial Finance*, 39(7), 2013, 667-676.
- [40] Kharkeshi, B.A., Mehregan, M., Sheykhi, M., *Sensitivity analysis of energy, exergy, and environmental models for a combined cooling, heating, and power system at different operating conditions of proton exchange membrane fuel cell*, *Environmental Progress & Sustainable Energy*, 2023, DOI: 10.1002/ep.14129.

## ORCID iD

Mohsen Zamani  <https://orcid.org/0009-0001-8573-039x>

Rouzbeh Shafaghat  <https://orcid.org/0000-0003-4827-5727>

Behrad Alizadeh Kharkeshi  <https://orcid.org/0000-0001-6522-6914>



© 2023 Shahid Chamran University of Ahvaz, Ahvaz, Iran. This article is an open access article distributed under the terms and conditions of the Creative Commons Attribution-NonCommercial 4.0 International (CC BY-NC 4.0 license) (<http://creativecommons.org/licenses/by-nc/4.0/>).

**How to cite this article:** Zamani M., Shafaghat R., Alizadeh Kharkeshi B. Numerical Study of the Hydrodynamic Behavior of an Archimedes Screw Turbine by Experimental Data in order to Optimize Turbine Performance: The Genetic Algorithm, *J. Appl. Comput. Mech.*, 9(4), 2023, 1060-1075. <https://doi.org/10.22055/jacm.2023.43137.4031>

**Publisher's Note** Shahid Chamran University of Ahvaz remains neutral with regard to jurisdictional claims in published maps and institutional affiliations.

